AIP Applied Physics Letters

Growth of (103) fiber-textured SrBi 2 Nb 2 O 9 films on Pt-coated silicon

G. Asayama, J. Lettieri, M. A. Zurbuchen, Y. Jia, S. Trolier-McKinstry, D. G. Schlom, S. K. Streiffer, J-P. Maria, S. D. Bu, and C. B. Eom

Citation: Applied Physics Letters **80**, 2371 (2002); doi: 10.1063/1.1463697
View online: http://dx.doi.org/10.1063/1.1463697
View Table of Contents: http://scitation.aip.org/content/aip/journal/apl/80/13?ver=pdfcov
Published by the AIP Publishing

Growth of (103) fiber-textured $SrBi_2Nb_2O_9$ films on Pt-coated silicon

G. Asayama, J. Lettieri, M. A. Zurbuchen, Y. Jia, S. Trolier-McKinstry, and D. G. Schlom[a)]
Department of Materials Science and Engineering, The Pennsylvania State University, University Park, Pennsylvania, 16803-6602

S. K. Streiffer
Materials Science Division, Argonne National Laboratory, Argonne, Illinois 60439

J-P. Maria
Department of Materials Science and Engineering, North Carolina State University, Raleigh, North Carolina 27695

S. D. Bu and C. B. Eom
Department of Materials Science and Engineering, University of Wisconsin–Madison, Madison, Wisconsin 53706-1687

(Received 28 August 2001; accepted for publication 1 February 2002)

(103) fiber-textured $SrBi_2Nb_2O_9$ thin films have been grown on Pt-coated Si substrates using a $SrRuO_3$ buffer layer. High-resolution transmission electron microscopy reveals that the fiber texture arises from the local epitaxial growth of (111) $SrRuO_3$ grains on (111) Pt grains and in turn (103) $SrBi_2Nb_2O_9$ grains on (111) $SrRuO_3$ grains. The films exhibit remanent polarization values of 9 $\mu C/cm^2$. The uniform grain orientation (fiber texture) should minimize grain-to-grain variations in the remanent polarization, which is important to continued scaling of ferroelectric memory device structures. © *2002 American Institute of Physics.* [DOI: 10.1063/1.1463697]

Since the discovery of high-fatigue resistance in bismuth-based layered ferroelectrics (Aurivillius phases[1]), and in particular $SrBi_2Nb_2O_9$ and $SrBi_2Ta_2O_9$,[2] these materials have been extensively investigated for ferroelectric random-access memory (FRAM) applications.[3] To achieve high-storage density with continued feature-size reduction, it is desired to prepare ferroelectric films in which the remanent polarization (P_r) is not only high, but also equal for every capacitor in the memory structure.

Previously, we reported[4] the growth of $SrBi_2Nb_2O_9$ thin films with a P_r of 15.7 $\mu C/cm^2$—over 25% higher than the highest reported value for randomly oriented polycrystalline $SrBi_2Nb_2O_9$ films.[5] These (103)-oriented $SrBi_2Nb_2O_9$ films were epitaxially grown on (111) $SrTiO_3$ substrates with (111)-oriented $SrRuO_3$ epitaxial bottom electrodes. Such ferroelectric capacitors have not only high P_r, but also uniform P_r across the entire film, since the film is epitaxial. Preparation of films with these desired ferroelectric properties have, however, required the use of small and costly single-crystal oxide substrates. Recently, the growth of non-c-oriented $SrBi_2Ta_2O_9$ epitaxial films on (100) Si substrates, including (103) $SrBi_2Ta_2O_9$ films, has been achieved using a sequence of intermediate epitaxial layers.[6,7] The P_r of the reported films on silicon has, however, been rather low: 5.2 $\mu C/cm^2$ in the best case.[7]

In this letter, we show that high P_r (and a concomitant uniformity in P_r) can be achieved on practical Pt-coated silicon substrates using local epitaxy to impart the (111) fiber texture of a platinum film into a fiber-textured (103) $SrBi_2Nb_2O_9$ film.

Previous research has shown that the fiber texture of Pt-coated silicon is not inherited by $SrBi_2Nb_2O_9$ or $SrBi_2Ta_2O_9$ films when they are grown directly on (111) fiber-textured platinum.[8,9] This is not surprising considering the differences in crystal structure, lattice constant, electronic structure, and especially the chemical reactivity of platinum with these bismuth-based compounds.[9–11]

Although randomly oriented polycrystalline $SrBi_2(Ta,Nb)_2O_9$ films are currently widely used for FRAMs, the P_r of each grain is different. This grain-to-grain variation in P_r results in severe nonuniformity in P_r as the capacitor area approaches the grain size,[12] which poses a technological scaling problem and results in the measured P_r (averaged over many grains) to be only about half as high as it could be in an optimally oriented $SrBi_2(Ta,Nb)_2O_9$ film.[13] In contrast to randomly oriented $SrBi_2Nb_2O_9$ films, however, the orientation perpendicular to the parallel-plate electrodes (for planar capacitor structures) is the same for all grains in epitaxial and fiber-textured films.

We have investigated the use of an intermediate layer to achieve orientation control in the growth of $SrBi_2(Ta,Nb)_2O_9$ films on Pt-coated silicon substrates. $SrRuO_3$ works well in this regard. It has an excellent lattice match to silicon (Pt has $a=3.924$ Å and $SrRuO_3$ has $a=3.925$ Å).[14,15] $SrRuO_3$ has been shown to grow in an oriented fashion on Pt-coated silicon substrates with (111) $SrRuO_3 \parallel$ (111) Pt.[16] As $SrRuO_3$ is conductive, its use as a buffer layer will not affect the hysteresis characteristics of the ferroelectric. Additionally, unlike the direct deposition of $SrBi_2(Ta,Nb)_2O_9$ on platinum, the strong chemical stability of the Pt/$SrRuO_3$ and $SrRuO_3/SrBi_2(Ta,Nb)_2O_9$ interfaces minimizes reaction between the platinum and $SrBi_2(Ta,Nb)_2O_9$ layers.

The means by which the (111) fiber texture of a Pt-coated silicon wafer can be used to impart (103) fiber texture

[a)]Electronic mail: schlom@ems.psu.edu

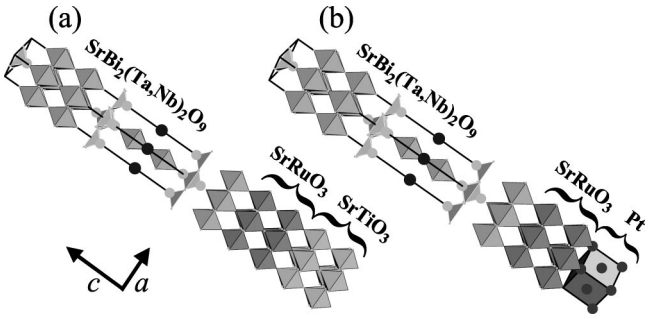

FIG. 1. Schematic showing (a) the established epitaxial orientation relationship of (103) $SrBi_2Nb_2O_9$ on (111) $SrRuO_3$ on (111) $SrTiO_3$ and (b) the local epitaxial relationship a top a single platinum grain for the growth of (103) fiber-textured $SrBi_2Nb_2O_9$ on (111) $SrRuO_3$ on (111) Pt-coated Si. The $SrBi_2Nb_2O_9$ is drawn and its unit cell is outlined in its tetragonal state above its Curie temperature. The direction of the *a* and *c* axes of $SrBi_2Nb_2O_9$ (below its Curie temperature) are indicated.

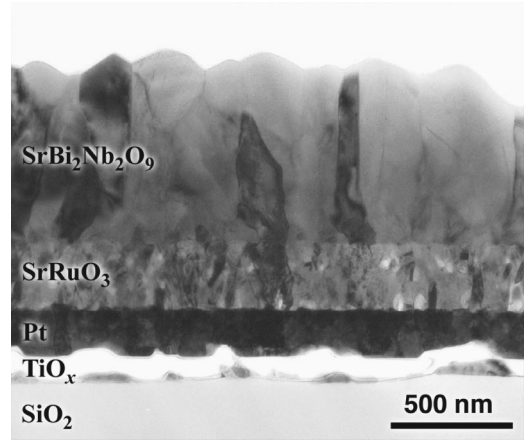

FIG. 2. Cross-sectional TEM image of a (103) fiber-textured $SrBi_2Nb_2O_9$/(111) fiber-textured $SrRuO_3$/(111) fiber-textured Pt/Ti/SiO_2/(100) Si film. The underlying (100) Si substrate is not shown.

on a $SrBi_2(Ta,Nb)_2O_9$ film is shown schematically in Fig. 1. The approach used is analogous to that demonstrated for the epitaxial growth of (103) $SrBi_2Nb_2O_9$ on (111) $SrTiO_3$ (also shown in Fig. 1)[4] with (111) Pt taking the place of (111) $SrTiO_3$. The epitaxial alignment shown takes place locally on each grain of (111)-oriented platinum in the (111) fiber-textured Pt-coated silicon film, leading to a fiber-textured (103) $SrBi_2Nb_2O_9$ film on a fiber-textured (111) $SrRuO_3$ film on the fiber-textured (111) Pt-coated silicon substrate. This approach is related to the perovskite ''template'' technique developed by Ramesh *et al.* for the growth of (001) fiber-textured ferroelectric[17] and colossal magnetoresistance[18] perovskite films on silicon substrates.

$SrRuO_3$ thin films were grown *in situ* by pulsed-laser deposition (PLD) using a KrF excimer laser (248 nm, Lambda Physik EMG 103MSC) in an on-axis geometry. The $SrRuO_3$ films were grown in 100 mTorr O_2 at 600 °C using a stoichiometric target. A laser pulse energy of 140 mJ, fluence of 2–3 J/cm^2, and a 5 Hz pulse rate were used to grow films about 0.3 μm thick. The same oxygen pressure used for growth was introduced as the Pt/Ti/SiO_2/(100) Si substrates were heated above ~350 °C to minimize titanium diffusion from the 20-nm-thick titanium adhesion layer into the platinum layer.[19–21] The $SrBi_2Nb_2O_9$ films were grown in 70 mTorr of mixed O_3/O_2 (~O_3 8%) at a substrate temperature of 874 °C. A laser pulse energy of 160 mJ, fluence of 2–3 J/cm^2, and a 4 Hz pulse rate were used to grow $SrBi_2Nb_2O_9$ films 0.5–0.75 μm thick. A single target with a Sr:Bi:Nb atom ratio of 1:2.3:2 was used as the source material. After growth, the films were quenched in 1 atm of oxygen. Details concerning target fabrication and optimization of the growth of these bismuth-based compounds are given elsewhere.[22]

Heterostructures composed of an overlying (103)-oriented fiber-textured $SrBi_2Nb_2O_9$ film on an underlying (111) fiber-textured $SrRuO_3$ electrode on a (111) fiber-textured 150 nm Pt/20 nm Ti/1 μm SiO_2/(100) Si substrate were prepared and investigated both structurally and electrically. For electrical measurements, 50 μm diam top platinum electrodes were deposited on the films through a shadow mask by e-beam evaporation. Ferroelectric hysteresis loops were traced out by stimulating the sample with a 20 kHz triangle wave (Tektronix AFG310), and collecting displacement current using a virtual ground current amplifier (Stanford Research Systems SR570). This current was integrated to yield the loop. By monitoring leakage current after switching had occurred and at the maximum electric field applied to the sample, it was verified that leakage contributed no more than 2–3 μC/cm^2 to the remanent polarization reported here. The high speed of the test compared to more standard methodologies was required to separate leakage and polar-

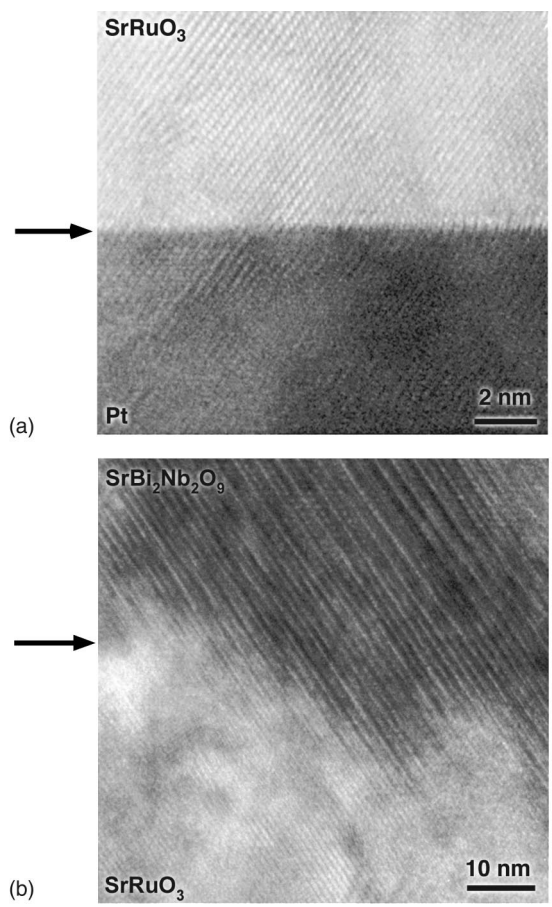

FIG. 3. HRTEM images of the interfaces (indicated by the position of the arrows) at either end of a single $SrRuO_3$ grain. (a) HRTEM image of the $SrRuO_3$/Pt interface and (b) HRTEM image of the $SrBi_2Nb_2O_9$/$SrRuO_3$ interface. The continuity in the lattice planes across the interfaces indicates that local epitaxy occurred. These HRTEM images are from the same film as the TEM image in Fig. 2.

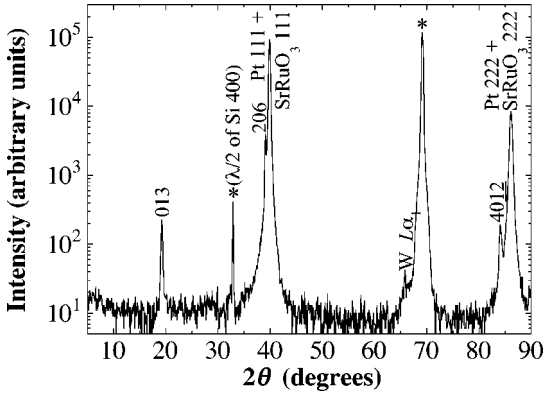

FIG. 4. θ–2θ x-ray diffraction scan of the same film on which the TEM image in Fig. 2 was made indicating that the $SrBi_2Nb_2O_9$ film is (103) oriented. The substrate peaks are labeled as (*).

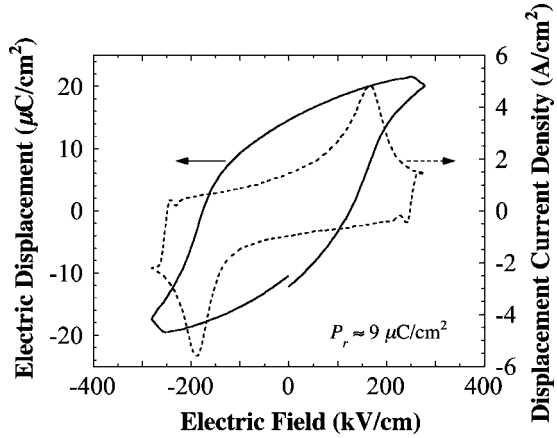

FIG. 5. Electric displacement–electric field hysteresis curve. The displacement current density–electric field response from which the hysteresis loop was generated is also shown.

ization contributions to the measured displacement current.

A cross-sectional TEM image of the entire (103) $SrBi_2Nb_2O_9$/(111) $SrRuO_3$/(111) Pt/Ti/SiO_2/Si heterostructure is shown in Fig. 2. The $SrBi_2Nb_2O_9$ layer consists of columnar grains with average diameters of about 150 nm. Higher-magnification images of the $SrBi_2Nb_2O_9$/$SrRuO_3$ and $SrRuO_3$/Pt interfaces of this same film by HRTEM reveal that local epitaxy occurred across both interfaces for each grain. This is manifested by the continuity of the lattice planes across both the $SrRuO_3$/Pt and $SrBi_2Nb_2O_9$/$SrRuO_3$ interfaces in Fig. 3. Through local epitaxy the underlying (111)-oriented $SrRuO_3$ grain in Fig. 3(a) has inherited its (111) orientation from the underlying platinum grain. Similarly, the $SrBi_2Nb_2O_9$ grain in Fig. 3(b) has inherited its (103) orientation from the underlying $SrRuO_3$ grain through local epitaxy. Local epitaxy was verified on multiple grains in the TEM and always had the orientation relationship shown in Fig. 1(b).

The occurrence of local epitaxy on a macroscopic scale was revealed by x-ray diffraction scans. The θ–2θ x-ray diffraction scan shown in Fig. 4(a) shows that globally the $SrBi_2Nb_2O_9$ layer is (103) textured and the platinum layer is (111) textured. The full width at half maximum (FWHM) of the 206 reflection of $SrBi_2Nb_2O_9$ is 0.24° and 2.60° in 2θ and ω, respectively. No peaks indicating other orientations of the $SrBi_2Nb_2O_9$, $SrRuO_3$, or platinum layers are seen in this scan. Note that the 111 and 222 $SrRuO_3$ peaks overlap the 111 and 222 Pt peaks. To confirm the macroscopic (111) texture of the $SrRuO_3$ layer, a χ scan of the 110 $SrRuO_3$ peak[15] was made and a clear peak with a FWHM of 4.0° in χ was observed. The 110 peak of platinum is forbidden, but is very intense for $SrRuO_3$, making this a good reflection to check the macroscopic orientation of the $SrRuO_3$ layer.

The electric displacement–electric field hysteresis of a (103)-oriented fiber-textured $SrBi_2Nb_2O_9$ film grown on Pt-coated silicon is shown in Fig. 5. The P_r and coercive field (E_c) were determined to be 9 μC/cm^2 and 150 kV/cm, respectively. Note that these results are for a relatively high-temperature deposition process (874 °C) optimized for epitaxial quality. Improvements in ferroelectric loop shape are expected from lower-temperature deposition processes.

The authors gratefully acknowledge the financial support of the National Science Foundation through Grant No. DMR-0103354 for the work performed at Penn State and Grant No. DMR-9973801 for the work performed at the University of Wisconsin, the U.S. Department of Energy through Contract No. W-31-109-ENG-38 for the work performed at ANL, and use of the ANL Electron Microscopy Center.

[1] B. Aurivillius, Ark. Kemi **1**, 463 (1950); **1**, 499 (1950); **2**, 519 (1951); **5**, 39 (1953); B. Aurivillius and P. H. Fang, Phys. Rev. **126**, 894 (1962).
[2] C. A-P. de Araujo, J. D. Cuchiaro, L. D. McMillan, M. C. Scott, and J. F. Scott, Nature (London) **374**, 627 (1995).
[3] O. Auciello, J. F. Scott, and R. Ramesh, Phys. Today **51**, 22 (1998).
[4] J. Lettieri, M. A. Zurbuchen, Y. Jia, D. G. Schlom, S. K. Streiffer, and M. E. Hawley, Appl. Phys. Lett. **75**, 2827 (1999).
[5] K. Watanabe, M. Tanaka, E. Sumitomo, K. Katori, H. Yagi, and J. F. Scott, Appl. Phys. Lett. **73**, 126 (1998).
[6] H. N. Lee, S. Senz, N. D. Zakharov, C. Harnagea, A. Pignolet, D. Hesse, and U. Gösele, Appl. Phys. Lett. **77**, 3260 (2000).
[7] H. N. Lee, S. Senz, A. Pignolet, and D. Hesse, Appl. Phys. Lett. **78**, 2922 (2001).
[8] J. S. Lee, H. H. Kim, H. J. Kwon, and Y. W. Jeong, Appl. Phys. Lett. **73**, 166 (1998).
[9] N. Fujimura, D. T. Thomas, S. K. Streiffer, and A. I. Kingon, Jpn. J. Appl. Phys., Part 1 **37**, 5185 (1998).
[10] C. D. Gutleben, Appl. Phys. Lett. **71**, 3444 (1997).
[11] Y. Shimakawa and Y. Kubo, Appl. Phys. Lett. **75**, 2839 (2000).
[12] A. Gruverman, Appl. Phys. Lett. **75**, 1452 (1999).
[13] T. Takenaka and K. Sakata, Jpn. J. Appl. Phys. **19**, 31 (1980).
[14] *Landolt-Börnstein: Numerical Data and Functional Relationships in Science and Technology*, edited by K.-H. Hellwege and A. M. Hellwege, New Series, Group III (Springer, Berlin, 1971), Vol. 6, p. 20; (Springer, Berlin, 1977), Vol. 7, Part f, p. 743.
[15] $SrRuO_3$ can be considered as a pseudocubic perovskite with $a \approx 3.925$ Å. Pseudocubic indexing is used throughout this manuscript for $SrRuO_3$.
[16] J. Yin, Z. G. Liu, and Z. C. Wu, Appl. Phys. Lett. **75**, 3396 (1999).
[17] R. Ramesh, T. Sands, and V. G. Keramidas, J. Electron. Mater. **23**, 19 (1994).
[18] J. Y. Gu, C. Kwon, M. C. Robson, Z. Trajanovic, K. Ghosh, R. P. Sharma, R. Shreekala, M. Rajeswari, T. Venkatesan, and R. Ramesh, Appl. Phys. Lett. **70**, 1763 (1997).
[19] J. O. Olowolafe, R. E. Jones, Jr., A. C. Cambell, R. I. Hegde, C. J. Mogab, and R. B. Gregory, J. Appl. Phys. **73**, 1764 (1993).
[20] K. Sreenivas, I. Reaney, T. Maeder, N. Setter, C. Jagadish, and R. G. Elliman, J. Appl. Phys. **75**, 232 (1994).
[21] J. Im, A. R. Krauss, A. M. Dhote, D. M. Gruen, O. Auciello, R. Ramesh, and R. P. H. Chang, Appl. Phys. Lett. **72**, 2529 (1998).
[22] J. Lettieri, Y. Jia, S. J. Fulk, D. G. Schlom, M. E. Hawley, and G. W. Brown, Thin Solid Films **379**, 64 (2000).